Fluorescence and mass spectrometry studies of the interaction between naproxen and synthetic pseudopeptidic models in organic media

M. Isabel Burguete [a], Ghinwa Fawaz [b], Francisco Galindo [a,*], M. Ángeles Izquierdo [a], Santiago V. Luis [a,*], Jean Martínez [b], Xavier J. Salom-Roig [b,*]

[a] Departamento de Química Inorgánica y Orgánica, Universitat Jaume I/CSIC Av. Sos Baynat, s/n, 12071 Castellón, Spain
[b] Institut de Biomolécules Max Mousseron (IBMM), UMR 5247, Synthèses Stéréosélectives, Place Eugène Bataillon, Université Montpellier II, France

ARTICLE INFO

ABSTRACT

Time-resolved/steady-state fluorescence and mass spectrometry measurements have shown the preferential binding of a non-steroidal anti-inflammatory drug (NSAID) like naproxen **4** to a synthetic pseudopeptidic receptor built using Phe (**9**), i.e., bearing an aromatic ring, compared to another model synthesized using Lys (**8**), i.e., lacking such aromatic ring but with a basic binding site. The quenching of the emission of naproxen by models **8** and **9** has been measured in solvents of different nature and analyzed by means of the Stern–Volmer methodology. In non-polar solvent (dichloromethane) the fluorescence of **4** is quenched to a higher extent by **8** than by **9** but in polar medium (methanol) the opposite occurs. The result in methanol is compatible with the existence of π–π stacking interactions between the aromatic rings of naproxen and the aromatic ring of **9**. In order to proof this model, mass spectrometry measurements have confirmed the higher stability of the complex formed by **4** and **9** over the related one formed with **8**. The observed phenomenon could help to understand the importance of aromaticity in the interactions between NSAIDs and more complex biological macromolecules like misfolded proteins, involved in the development of Alzheimer's disease and other neuropathologies.

1. Introduction

Neuropathologies are important health problems for modern societies. Quite a number of them are linked to protein misfolding. One of the paradigmatic examples is the Alzheimer's disease (AD),[1-4] which is characterized by deposits of β-amyloid (Aβ) peptides in the brain. Despite the enormous efforts made to elucidate the mechanism of the genesis of the AD, there are still open questions that are a challenge for a broad array of scientific disciplines.[5-10] Much effort is currently being carried out to design new molecules capable to interrupt the self-assembly process. But the development of new β-blockers is hampered by the lack of a fundamental knowledge about the mode of action of such ligands. Studies using molecules targeting directly β-amyloid derivatives have provided some clues about the molecular mode of interaction between exogenous ligands and misfolded proteins.[11-15] Thus, different binding sites have been identified through the use of distinct imaging tracers like Congo Red (**1**), Thioflavin T (**2**) and FDDP (**3**) (Chart 1).[16-20] In this
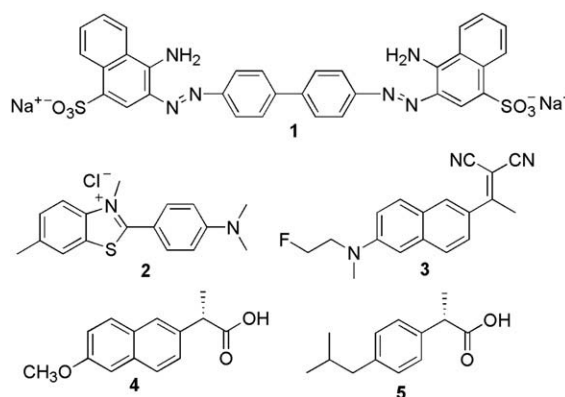

Chart 1. Some molecules capable to bind amyloid aggregates.

regard, non-steroidal anti-inflammatory drugs (NSAID) like naproxen (**4**) and ibuprofen (**5**) have been found to displace the hydrophobic probe **3** from the plaques of AD brain specimens,[21] which suggests *hydrophobic rather than ionic* interactions as driving forces for the stacking of such NSAIDs to fibrils, also supporting the anti-amyloidogenic properties of NSAIDs.[22-25]

* Corresponding authors. Tel.: +34 964728239; fax: +34 964728214.
E-mail addresses: francisco.galindo@uji.es (F. Galindo), luiss@uji.es (S.V. Luis), salom-roig@univ-montp2.fr (X.J. Salom-Roig).

The above-cited studies use complex chemical systems (amyloid fibrils, synthetic polypeptides, etc.) and indirect measurements like displacement assays. In order to understand more precisely the intermolecular interactions between NSAIDs and pathogenic fibrils it would be useful to simplify the peptide system under study by means of models mimicking specific features of fibrils or polypeptides. One of the key issues to study in order to approach this challenging problem is to disclose the chemical nature of the interactions (H-bonding, π-stacking, ion–ion, ion–dipole, etc.) taking place when a certain NSAIDs interacts with a certain misfolded protein or, even better, with shorter peptides prone to aggregation (for instance the well known Lys-Leu-Val-Phe-Phe). Two extreme models can be considered for such interactions between peptides and 2-arylpropionic NSAIDs: one in which ionic forces predominate (through salt bridges between carboxylates of the drug and cationic residues of the peptide receptor, like Lys) and another in which solvophobic forces control the binding between NSAIDs and the peptidic system. However, to discern clearly both contributions studying a complex peptidic-NSAID assembly in a natural aqueous environment is extremely difficult, and simplified models are needed.

The objective of the present study is to demonstrate the importance of π-stacking interactions in the supramolecular recognition of naproxen by synthetic receptors of pseudopeptidic nature. For such purpose two models have been constructed, differing in the nature of one building block. Whereas one receptor has been made using Lys, and hence is carrying a basic residue, the other one has been made using Phe, and thus contains an aromatic ring. From the analysis of the static and dynamic quenching of the fluorescence of **4** it is demonstrated that the neutral aromatic derivative binds naproxen in polar medium (methanol) stronger that the basic synthetic model. Confirmatory evidence by mass spectrometry has also been obtained. The aim of this study is not to emulate the behaviour of misfolded peptides leading to pathological states, which is a challenging issue, but to approach the phenomenon of aromatic–aromatic interactions by using fluorescence techniques, especially in the time-resolved mode, and under controlled conditions (organic media).

2. Results and discussion

In order to design the pseudopeptides capable to distinguish between ionic and aromatic interactions, it was decided to synthesize two dyads comprised by two amino acids, one amino acid capable to perturb the fluorescence of naproxen, and another amino acid with basic or aromatic features. Hence dyads **8** and **9** (Chart 2), containing Trp (as quencher of **4** likely via electron-transfer or exciplex formation) linked by ethylenediamine to either Lys (in **8**) or Phe (in **9**), were envisaged as potential receptors for naproxen, enhancing the ionic or aromatic–aromatic interactions, respectively. Prior to synthesize the mentioned receptors, it was

checked that the Trp subunit by itself was capable to quench the emission of **4**, by means of control experiments with *tert*-butyloxycarbonyl tryptophan (BOC-Trp, **6**) and carbobenzyloxy tryptophan (Cbz-Trp, **7**), as will be shown later.

2.1. Synthesis

Synthetic compounds **8** and **9** were prepared by coupling of ethylendiamine to both amino acids forming each dyad (Trp and Lys, or Trp and Phe) in a sequential manner, as indicated in Scheme 1. Thus, starting from the Boc-protected aminoacid (Lys or Phe), in the presence of PyBOP, HOBt and DIEA in anhydrous DMF,[26–28] intermediates **10** or **11** were obtained completely free of the diacetylated C_2 symmetry derivative. Successive coupling of the remaining free amine end with BocTrp yielded model compound **9** and intermediate **12**. For the latter, selective deprotection of the Cbz group by means of H_2/Pd–C led to model compound **8**. All the products were characterized unambiguously by means of ^{1}H and ^{13}C NMR, ESI-MS, FABMS and HRMS (see Experimental section). This synthetic approach constitutes a variation over the series of C_2 symmetric pseudopeptides reported by our group.[29–32]

2.2. Fluorescence measurements

The fluorescence of naproxen was measured in both polar (methanol, MeOH) and apolar (dichloromethane, DCM) solvents. The extent of the intermolecular quenching of the fluorescence of **4** by pseudopeptides **8** and **9** can be correlated with the extent of the binding and hence, with the relative importance of the aromatic (**9**) and the ionic (**8**) contributions for such interaction. In all the cases, the corresponding control experiments with **6** and **7** were carried out. The pseudopeptides here employed allowed reproducible measurements in both methanol and dichloromethane, which allows obtaining a more complete picture of the supramolecular binding. Quenching experiments were attempted with commercial dipeptides (TrpLys, TrpPhe) in water but the results were hardly reproducible, most likely due to protonation processes leading to several species coexisting in solution. On the other hand, the utilization of buffers resulted in the introduction of additional variables, adding complexity to the analysis. Therefore, we decided to study compounds **8** and **9** in model solvents such as MeOH and DCM.

A simple mathematical model describing the fluorescence of a molecule participating in an intermolecular quenching process is that in which the probe molecule is quenched as a result of (a) ground-state complexation or (b) collision during the lifetime of the excited probe.

$$I_0/I = 1 + K_1[Q] \tag{1}$$

$$\tau_0/\tau = 1 + K_2[Q] \tag{2}$$

If the quenching occurs only as a consequence of the collision of the chemical species during the lifetime of the excited probe (*dynamic quenching*), the situation can be analyzed by means of the Stern–Volmer relationships: Eq. 1 (where I_0 and I are the fluorescence intensities of the fluorescent probe in the absence and in the presence of quencher (Q), respectively) and Eq. 2 (in which τ_0 and τ are the lifetimes of the probe in the absence and in the presence of Q, respectively).[33] If the quenching is purely dynamic then $I_0/I = \tau_0/\tau$, and hence $K_1 = K_2$. A completely different situation occurs when the quenching occurs only as a result of a ground-state complexation. Then, the measured lifetimes are not affected by the quencher concentration, in such a way that $\tau_0/\tau = 1$, $K_2 = 0$, and K_1 reflects the association constant in the ground state (*static* quenching). In many instances both situations coexist, and specific equations have been
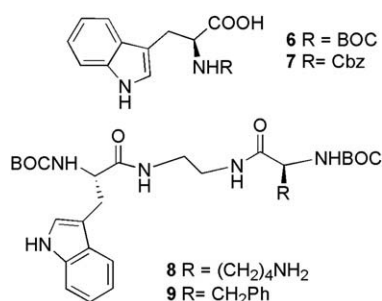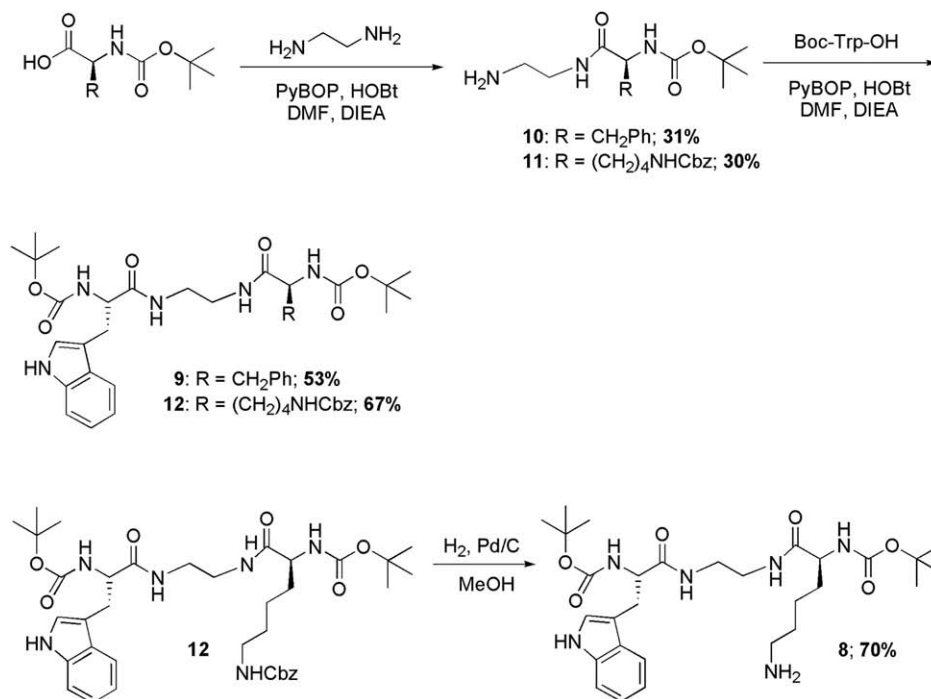

Chart 2. Model compounds (**6**, **7**) and synthetic pseudopeptides (**8**, **9**).

Scheme 1. Synthetic steps for the chemical preparation of receptors **8** and **9**.

developed to distinguish the dynamic and static contributions.[33–38] However, it is not always possible to apply accurately such models, and then the data can be analyzed by simplified Eqs. 1 and 2, K_2 affording the dynamic quenching and K_1 *reflecting* a combination of static and dynamic processes. The closer K_1/K_2 ratio to unity, the lower the complexation in the ground state would be. Although this kind of analysis is estimative, it can provide, along with additional techniques, an indication of the degree of complexation in systems where supramolecular binding constants cannot be obtained in other way because of low association constants, low sensitivity of the employed techniques, etc.

We have applied Eqs. 1 and 2 to fit the experimental quenching of the emission of **4** by **8** and **9**, to ascertain which mode of quenching predominates (dynamic or static) and to know indirectly, which quencher binds **4** in a higher extent. Thus, K_1 and K_2 for **8** and **9** were extracted by fitting the experimental data of steady-state (I_0/I) and time-resolved (τ_0/τ) emissions to Eqs. 1 and 2. The reference compounds containing only the indole moiety (**6** and **7**) were used as controls.

Naproxen is a fluorescent drug emitting at 352 nm when excited at 331 nm both in MeOH and DCM.[39,40] Steady-state fluorescence spectra of **4** in both solvents can be seen in Figure 1. The lifetimes of naproxen in these solvents in the absence of quencher resulted 5.5 ns (DCM) and 9.3 ns (MeOH), in close agreement with the literature data.[41,42]

Controlled amounts of quenchers **6**–**9** were added to solutions of pure naproxen in either DCM or MeOH, and the steady-state emission and fluorescence lifetimes were recorded. For illustrative purposes, the static and dynamic data for **4** quenched by reference **6** in methanol are shown in Figure 2.

Since the Trp chromophore is a potential fluorescent element, the wavelength at 331 nm was selected to excite selectively the naproxen.[43] Additionally, in order to prevent inner filter effects, all the measurements were done in the front-face configuration of the equipment. As it can be seen in Figure 2 for **6** and **4**, the fluorescence decays of **4** resulted monoexponential even in the presence of ca. 0.15 M of Boc-Trp, which indicates the absence of emission from the quencher under the excitation conditions.

The analysis of the 16 quenching experiments was performed by means of the Stern–Volmer equations to yield the fittings shown in Figure 3. The constants associated to these analyses are reported in Table 1.

The examination of data in Table 1 allows several conclusions. Compounds **6** and **7** provide the reference values for the analysis. The fact that both **6** and **7** present similar K_1 and K_2 in methanol means that the fluorescence quenching of **4** by such compounds is practically dynamic (ratio $K_1/K_2 \sim 1.0$–1.1). The same compounds in a non-polar solvent afforded some degree of association, with $K_1/K_2 \sim 1.4$–1.5. On the other hand, the peptidomimetic compounds containing Lys and Phe displayed higher values of the K_1/K_2 ratio than **6** and **7** in both solvents, indicating stronger binding, especially for **8** in DCM (6.9) and for **9** in MeOH (4.2). The binding affinity of the Lys containing model **8** in DCM is not surprising providing that the carboxylic acid and the amine of the side chain would form a strong salt bridge. However, compound **9** with the aromatic side chain of Phe displays elevated values of K_1/K_2 in both DCM (3.2) and MeOH (4.2). In fact, among the values in methanol, the ratio K_1/K_2 for **9** is remarkably high when compared to the rest of values in the same solvent. Indeed, this can be appreciated graphically in Figure 3c for the fitting with the higher slope. Additionally, the ratio for **8** in methanol results remarkably lower (1.5) than for **9** (4.2), which also supports the higher association of naproxen with **9** in polar solvent. This suggests that in MeOH a strong participation of the aromatic rings in the intermolecular association with the NSAID.

2.3. Mass spectrometry

The fluorescence measurements provide an array of data that analyzed by means of the Stern–Volmer methodology suggest the higher stability of the complex formed by **9** and naproxen in MeOH. Mass spectrometry measurements provided additional experimental evidence supporting this model. The study of supramolecular complexes in the gas phase is, in fact, the method of choice when the objective is to suppress any secondary effects caused by solvent in the complexation process (solvation/desolvation
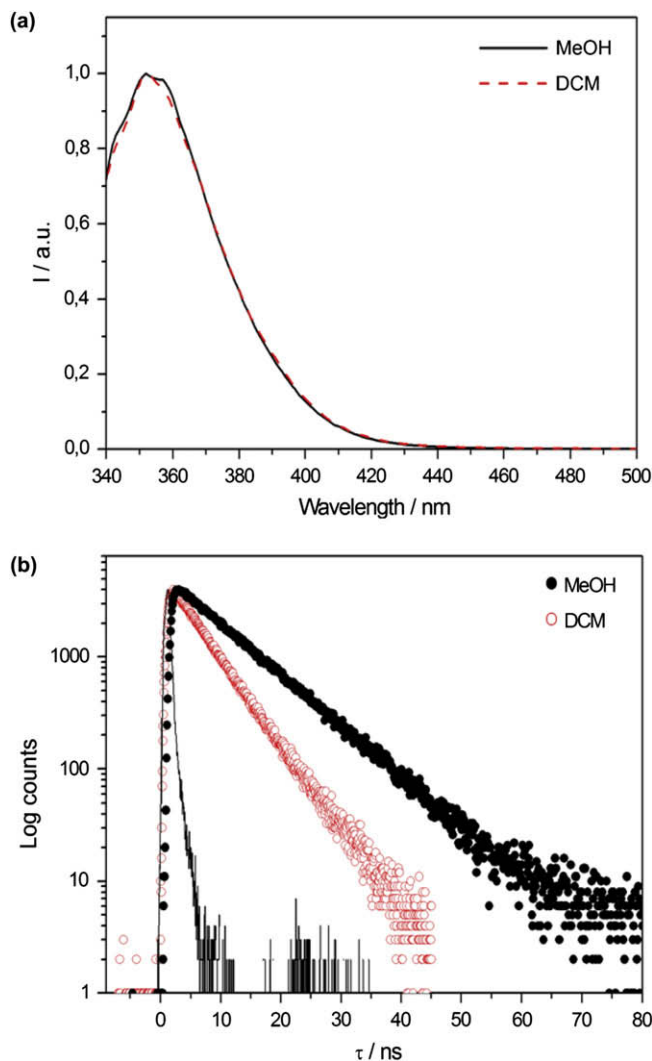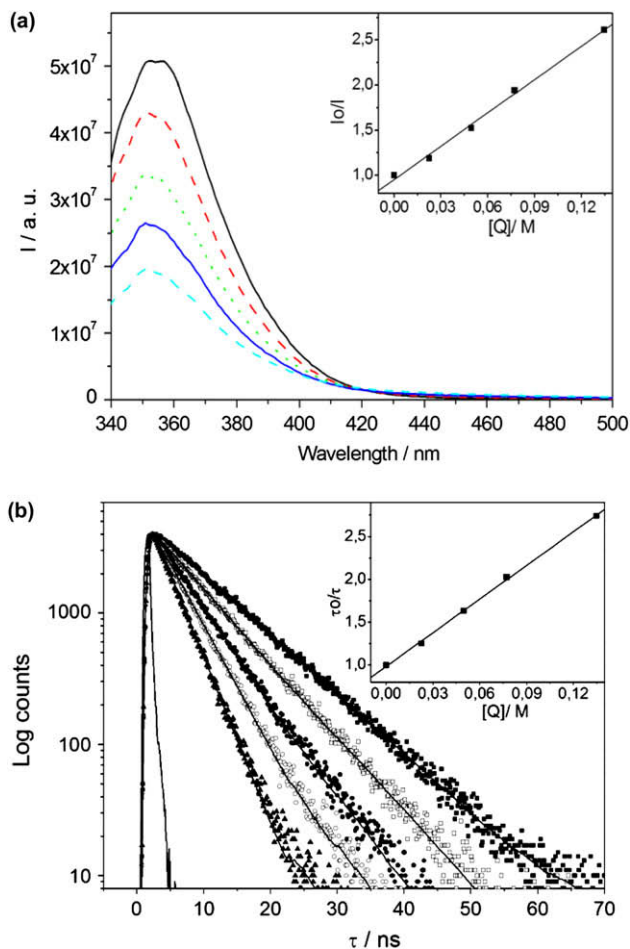
Figure 1. (a) Steady-state fluorescence spectra (λ_{exc}=331 nm) and (b) time-resolved fluorescence decays (λ_{exc}=325 nm, λ_{em}=350 nm) of **4** in DCM (red) and MeOH (black).


Figure 2. Representative quenching of the fluorescence of **4** by **6** in MeOH: (a) steady-state (λ_{exc}=331 nm) and (b) time-resolved (λ_{exc}=325 nm, λ_{em}=350 nm) measurements.

changes, etc.). As it has been shown in the literature, the comparative study of complexes in the gas phase affords precise information on the relationships between the structure of the model and the ligand compound and the stability of such complexes, without potential interferences by the surrounding environment. Mass spectrometry has been used frequently as analytical tool in such conditions,[44] along with other techniques.[45]

In the case of naproxen and compounds **8** and **9** the electrospray ionization-mass spectrometry (ESI-MS) experiments afforded, firstly, the unambiguous evidence of the existence of the postulated complexes. Mixtures of **8** or **9** in the presence of **4** in MeOH yielded peaks at *m/z* 827.4 and *m/z* 846.4, which is compatible with [**4**+**8**+Na]$^+$ and [**4**+**9**+Na]$^+$ species, respectively (Fig. 4).

In order to get a quantitative estimation of the strength of the binding, *collision induced dissociation* (CID) experiments were performed.[46–48] Those experiments confirmed the higher stability of complex formed between **4** and the Phe-contaning compound **9**. Upon CID conditions, the supramolecular singly charged [**4**+(**8** or **9**)+Na]$^+$ cation readily expels the ligand **4** leading to the [(**8** or **9**)+Na]$^+$ cation (Fig. 5).

A plot of the intensity percentage of a certain ion versus the collision energy allows a quantitative estimation of the gas-phase stability of the complex. We choosed the collision energy in the centre-of-mass frame necessary for 50% dissociation (E_{CM50}) as

a direct estimation of the gas-phase stability.[49] Thus, the ion at *m/z* 827.4, corresponding to the complex of naproxen with **8**, required 0.167 eV to reduce its intensity 50%, whereas the ion *m/z* 846.4 (for **9**) needed 0.175 eV to experience the same dissociation. As can be seen from the data of Figure 6, the curve for the complex between **9** and **4** reflects unequivocally the higher stability of this species, when compared to the one formed between **8** and **4**, in all the collision energy range.

This result, combined with the fluorescence measurements, confirms the preferential binding of naproxen to the receptor containing an aromatic ring (from Phe) over the one with the amine residue (from Lys). The supramolecular complex formed between naproxen and models **9** should be stabilized by a combination of weak interactions, not only by means of π-stacking, since the occurrence of π-stacking interactions in systems without conformational restrictions is very rare.[50–55]

3. Conclusions

Extrapolation of the conclusions here presented to the behaviour of systems with higher complexity like amyloid peptide must be done with caution since this study has been done with *model* compounds and under *model* conditions. However, we must remark the necessity of studies in controlled conditions, where the possibility of experimental artifacts is minimal, in order to progress in the basic knowledge of fundamental questions.[39] For instance, in water under physiological conditions **4** should be mostly unprotonated
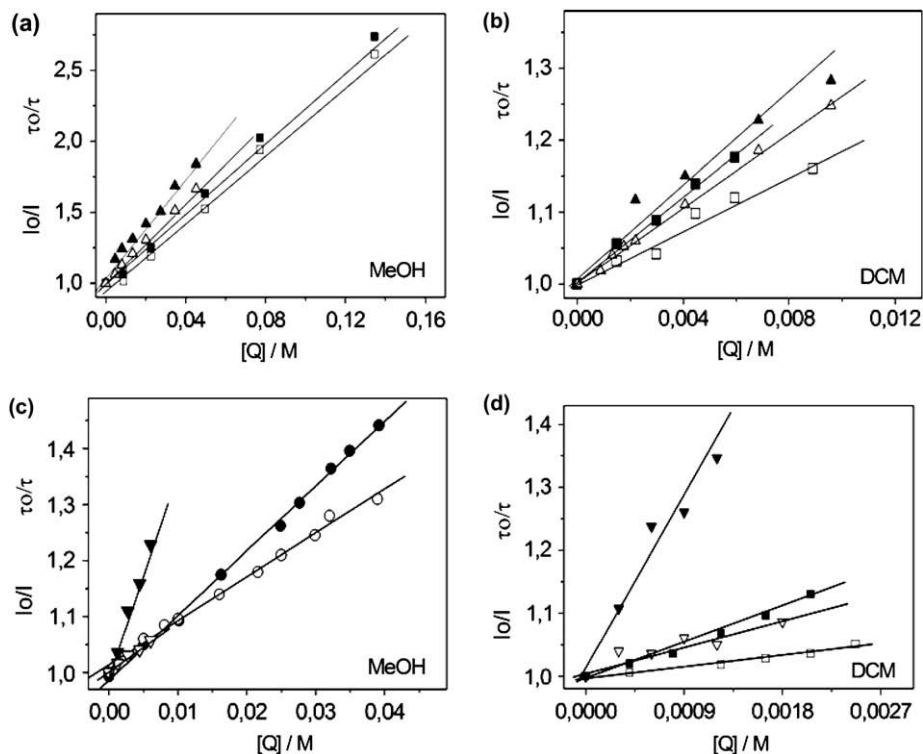
Figure 3. (a,b) Fluorescence quenching of **4** by **6** (squares) and **7** (up triangles). Steady-state (black) and time-resolved measurements (white). (c, d) Fluorescence quenching of **4** by **8** (circles) and **9** (down triangles). Steady-state (black) and time-resolved measurements (white).

Table 1
Stern–Volmer constants corresponding to the fluorescence quenching of **4** by compounds **6–9** in polar and apolar solvents

Solvent	Compound	K_1 (M^{-1})	K_2 (M^{-1})	K_1/K_2
MeOH	**6**	12 ± 1	12 ± 1	1.0
	7	17 ± 1	15 ± 1	1.1
	8	12 ± 1	8 ± 1	1.5
	9	38 ± 2	9 ± 1	4.2
DCM	**6**	29 ± 1	19 ± 2	1.5
	7	27 ± 2	20 ± 1	1.4
	8	282 ± 30	41 ± 9	6.9
	9	63 ± 4	20 ± 2	3.2

due to its acidic pK_a, which would be considered for future studies with water-soluble pseudopeptides. Nevertheless, under model conditions the higher binding affinity of **9** towards **4** (both in MeOH and in the gas phase) could indirectly support the occurrence of $\pi-\pi$ stacking interactions also between the aromatic rings in more complex systems, as it has been demonstrated to occur between aromatic β-blockers of fibrilar aggregation. In fact, hydrophobicity of some peptidic structures has been demonstrated to be a key factor to explain their aggregation properties and, consequently, aromatic inhibitors have been designed to stop the self-assembly process.[11–15,56–63] Gosh and co-workers have designed a polypeptide enriched with aromatic residues, capable to inhibit efficiently the β-amyloid fibrillization.[64] On the other hand, Gazit and co-workers have demonstrated the importance of aromaticity of some polyphenols (rather than their antioxidant properties) to explain their anti-aggregation properties.[65] Moreover, although the presence of aromatic moieties is not a requisite for amyloid assembly, it influences markedly in the kinetics of fibril formation.[66]

In summary, time-resolved/steady-state fluorescence and mass spectrometry measurements have demonstrated the preferential supramolecular binding of naproxen to a synthetic receptor built with Phe, as compared to another model synthesized with Lys.
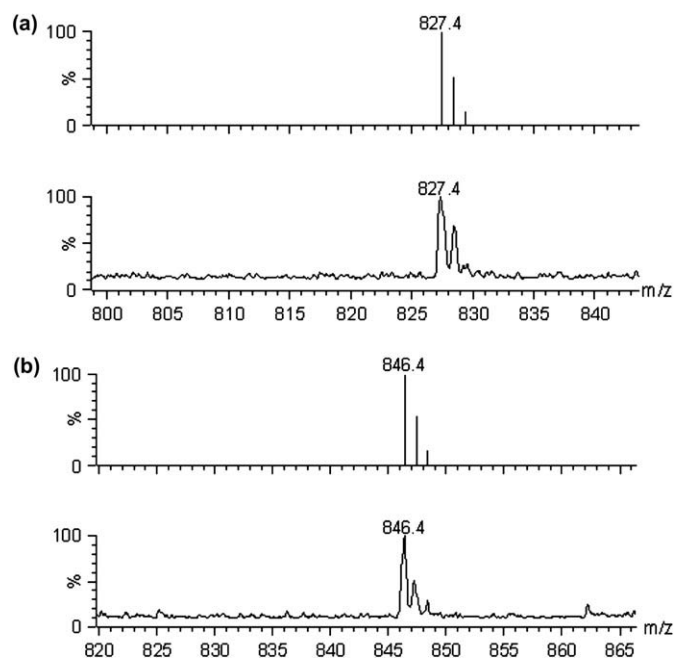
Figure 4. ESI-MS spectra: (a) **4** and **8** in MeOH (top: simulated, bottom: experimental); (b) **4** and **9** in MeOH (top: simulated, bottom: experimental).

4. Experimental section

4.1. Materials

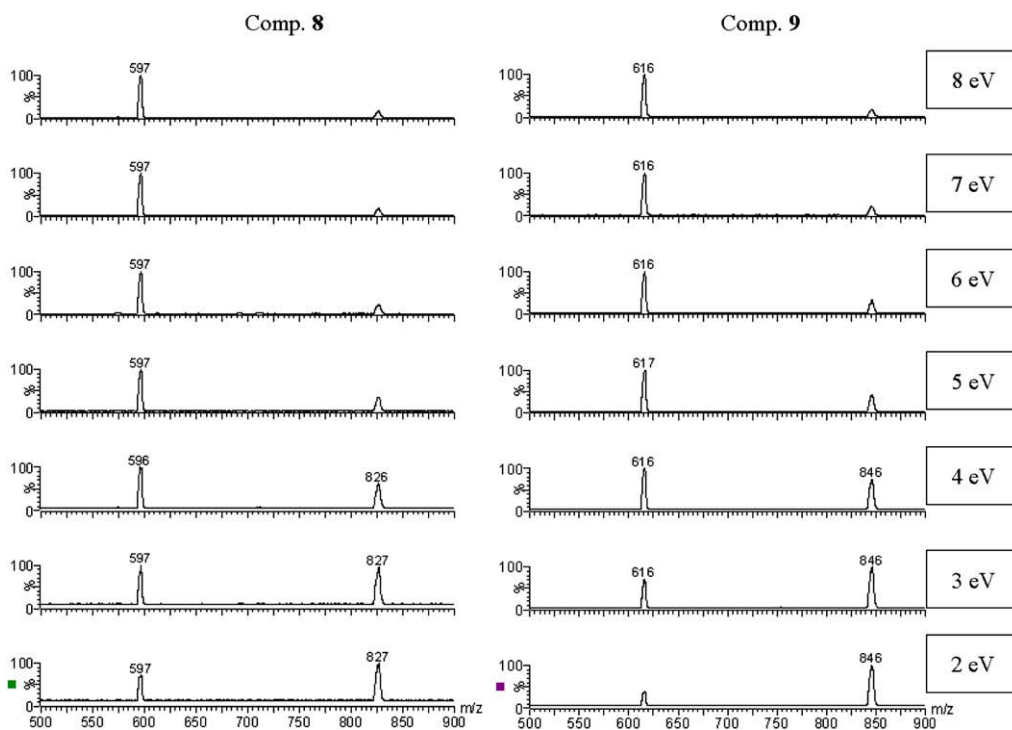**Figure 5.** Representative CID spectra in the E_{lab}=2–8 eV range for the mass-selected $[4+8+Na]^+$ (left) and $[4+9+Na]^+$ (right).
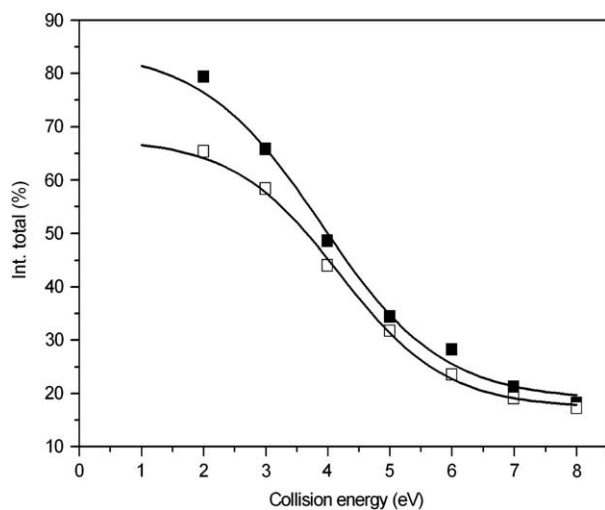

Figure 6. Collision induced dissociation performed on complexes formed by **4** with **8** (white squares) and **4** with **9** (black squares).

ethylenediamine, DIEA, DMF (spectroscopy grade) were purchased from Aldrich; methanol (spectroscopy grade, Scharlau). Dichloromethane was distilled over CaH_2 previous use.

4.2. Instrumentation

^{1}H and ^{13}C NMR analyses were performed with a Bruker Avance AM300 MHz and are reported in parts per million and calibrated using residual undeuterated solvents as the internal reference. Data are reported as: br=broad, s=singlet, d=doublet, t=triplet, q=quartet, m=multiplet; coupling constant(s) in hertz, integration.

Mass spectra (electrospray ionization mode, ESIMS) were recorded on a Platform II (Micromass) quadrupole mass spectrometer fitted with an electrospray interface. The mass

spectrometer was calibrated in the positive- and negative-ion ESI mode. The samples were dissolved in H_2O/CH_3CN (50/50 v/v). For the CID experiments a Quattro LC (QhQ quadrupole–hexapole–quadrupole) mass spectrometer with an orthogonal Z-spray-electrospray interface (Waters) was used. Sample solutions (ca. 1×10^{-4} M) in methanol were introduced through a fused-silica capillary to the ESI source via a syringe pump at a flow rate of 10 μL/min. The drying gas as well as nebulizing gas was nitrogen at a flow of 400 L/h and 70 L/h, respectively. The temperature of the source block was set to 80 °C and the interface to 120 °C. The capillary voltage was set at 3.5 kV in the positive scan mode and the cone voltage was adjusted (typically U_c 15 V) to control the extent of fragmentation in the source region. The chemical composition of each peak obtained in the full scan mode was assigned by comparison of the isotope experimental and theoretical patterns using the MassLynx 4.1 program.

FAB mass spectra and HRMS (High Resolution Mass Spectrum) were recorded on a JEOL JMS DX300-SX 102 in positive mode using NBA (3-nitrobenzylalcohol) or GT (mixture of glycerol/thioglycerol 50/50 v/v) as matrix.

Collision induced dissociation (CID) experiments were performed with argon at various collision energies, in the range of E_{lab}=0–15 eV. The collision gas pressure was maintained at approximately 4×10^{-4} mbar. The most intense precursor peak of interest was mass-selected with Q1, interacted with argon in the hexapole cell while scanning Q2 to monitor the ionic fragments. The resolution setting in Q1 (isolation width 3 u) and Q2 was low, in order to obtain a good signal-to-noise ratio. For a qualitative analysis of the energy-dependent CID experiments, the laboratory collision energies (E_{lab}) were converted to the centre-of-mass frame, $E_{CM}=m/(m+M)E_{lab}$, where m and M stand for the masses of the collision gas and the ionic species, respectively. For the breakdown profiles representation, signal intensities were obtained from the average of 40 scans and measuring the area of the fragmentation peaks. These graphs were represented taking into account the relative abundance of the precursor and product peaks of each compound ($I_{precursor\ ion}$ or $I_{product\ ion}/I_{precursor\ ion}+\sum I_{product\ ion}$)

against E_{CM}. We selected the value of the collision energy required for 50% reduction of the precursor ion ($E_{CM50\%}$) as a qualitative measure of the gas-phase stability.

Melting points were measured on a Büchi Melting Point 510 apparatus and are uncorrected.

Analytical high performance liquid chromatography (HPLC) was performed on a Waters Millenium 717 equipped with Autosampler, with a variable wavelength diode detector using a CHROMOLITH RP18 column (50×4.6 mm), flow 5 mL/min, linear gradient CH_3CN in water 0–100% (+0.1% TFA) in 4.5 min.

UV–vis absorption measurements were made using a Hewlett-Packard 8453 spectrophotometer.

Steady-state fluorescence spectra were recorded in a Spex Fluorog 3-11 equipped with a 450 W xenon lamp. Time-resolved fluorescence measurements were done with the technique of time correlated single photon counting (TCSPC) in an IBH-5000U. Samples were excited with a hydrogen nanosecond flash lamp. Data were fitted to the appropriate exponential model after deconvolution of the instrument response function by an iterative deconvolution technique, using the IBH DAS6 fluorescence decay analysis software, where reduced χ^2 (values between 0.90–1.19) and weighted residuals serve as parameters for goodness of fit.[40] All the samples were measured in aerated conditions.

Fluorescence was measured in the absence and in the presence of quencher. For the fluorescence titrations, 4 mL of naproxen solution (2–25)×10^{-5} M were placed in a fluorescence cell equipped with a Teflon stopper and a magnetic stirrer. The solution was titrated with successive additions of the quencher. The final concentrations of quenchers were 0.15 M (MeOH) or 0.01 M (DCM). After each titration the fluorescence spectra and the lifetimes were recorded. For the steady-state measurements, the excitation wavelength was set at 331 nm and the maximum value at 350 nm was taken as a measure of fluorescence intensity. For the time-resolved measurements, samples were excited at 325 nm and emission was monitored at 350 nm.

4.3. General procedure for the synthesis of monoacylated diamines 10 and 11

Ehtylenediamine (10 equiv) was suspended in DMF. Diisopropylethylamine (2 equiv) was added, followed by the appropriate Boc-protected aminoacid (1 equiv), 1-hydroxybenzotriazole (HOBt, 2 equiv) and PyBOP (1 equiv). The reaction was allowed to proceed at room temperature until judged complete by HPLC, typically 24–30 h. DMF was then removed by evaporation under reduced pressure and the resultant residue was suspended in ethyl acetate and treated with an aqueous saturated solution of $NaHCO_3$. Phases were separated and the aqueous one extracted with ethyl acetate. The organic layers were dried over magnesium sulfate and rotary evaporated to produce a crude yellow oil which was purified by column chromatography (silica, CH_2Cl_2/MeOH 4:1).

4.3.1. N^1-(2-Aminoethyl)-N-(tert-butoxycarbonyl)-L-phenylalaninamide (10)

1,2-Ethanediamine (5 mL, 0.076 mol), 2.6 mL (15.1 mmol) of DIEA, 2 g (7.55 mmol) of Boc-phenylalanine, 2.04 g (15.1 mmol) of HOBt and 3.93 g (7.55 mmol) of PyBOP in 50 mL DMF yielded 0.72 g (31%) of 10 as a white solid. Mp >260 °C; ^{1}H NMR (300 MHz; CDCl$_3$) δ 8.15–8.11 (m, 1H), 7.47 (br, 2H), 7.34–7.21 (m, 5H), 7.01 (d, 2H, J=6 Hz), 4.16–4.13 (m, 1H), 3.34–3.27 (m, 2H), 3.03 (dd, 1H, J′=15 Hz, J″=3 Hz), 2.84–2.76 (m, 3H), 1.34 (s, 9H); ^{13}C NMR (300 MHz; DMSO-d_6) δ 172.3, 155.2, 137.9, 129.1, 128.0, 126.2, 78.3, 55.7, 38.7, 37.4, 36.7, 28.0; ESIMS m/z 308.3 [M+H]$^+$; FAB(+) m/z 308.3 [M+H]$^+$; HRMS calcd for $C_{21}HN_4O_5$ [M+H]$^+$: 308.1974, found 308.1976.

4.3.2. N^1-(2-Aminoethyl)-N^6-[(benzyloxy)carbonyl]-N^2-(tert-butoxycarbonyl)-L-lysinamide (11)

1,2-Ethanediamine (7.0 mL, 0.105 mol), 3.7 mL (21.0 mmol) of DIEA, 4.0 g (10.5 mmol) of Boc-(Z)-lysine, 2.84 g (21.0 mmol) of HOBt and 5.47 (10.5 mmol) of PyBOP in 150 ml DMF yielded 1.32 g (30%) of 11 as a colourless oil. ^{1}H NMR (300 MHz; CDCl$_3$) δ 7.34–7.25 (m, 5H), 7.04 (br, 1H), 5.50 (br, 1H), 5.25 (br, 1H), 5.07 (s, 2H), 4.07–4.01 (m, 1H), 3.32–3.13 (m, 4H), 2.79 (t, 2H, J=6 Hz), 2.33 (br, 2H), 1.85–1.30 (m, 6H), 1.37 (s, 9H); ^{13}C NMR (300 MHz; CDCl$_3$) δ 173.1, 157.1, 156.3, 136.9, 128.9, 128.4, 80.4, 77.6, 70.0, 53.4, 33.2, 32.4, 29.7, 28.7, 26.2, 25.5, 22.9; ESIMS m/z 423.3 [M+H]$^+$; FAB(+) m/z 423.4 [M+H]$^+$; HRMS calcd for $C_{21}HN_4O_5$ [M+H]$^+$: 423.2607, found 423.2589.

4.4. General procedure for the synthesis of asymmetric diacylated diamines 9 and 12

The monoacylated diamine (1 equiv) was dissolved in DMF. To the resultant solution were added DIEA (2.2 equiv) followed by the Boc-protected tryptophan (1.1 equiv), 1-hydroxybenzotriazole (HOBt, 2.2 equiv) and PyBOP (1.1 equiv). The reaction was allowed to proceed at room temperature until judged complete by HPLC, typically 24–30 h. DMF was then removed by evaporation under reduced pressure and the resulting residue was suspended in ethyl acetate and treated with an aqueous saturated solution of $NaHCO_3$. Phases were separated and the aqueous one extracted with ethyl acetate. The organic layers were dried over magnesium sulfate and rotary evaporated to produce a crude yellow oil, which was purified by column chromatography (silica, CH_2Cl_2/MeOH 4:1).

4.4.1. N-(tert-Butoxycarbonyl)-N-(2-ethyl)-L-tryptophanamide (9)

Compound 10 (0.60 g, 1.95 mmol), 0.75 mL (4.29 mol) of DIEA, 0.65 g (2.15 mmol) of Boc-tryptophan, 0.58 (4.29 mmol) of HOBt and 1.12 g (2.15 mmol) of PyBOP in 22 mL DMF yielded 0.61 g (53%) of 9 as a white solid. Mp 178–180 °C; ^{1}H NMR (300 MHz; DMSO-d_6) δ 10.84 (br s, 1H), 7.99 (br s, 2H), 7.62 (d, 2H, J=9.0 Hz), 7.37–6.98 (m, 9H), 6.90 (d, 1H, J=9.0 Hz), 6.75 (d, 1H, J=6 Hz), 4.18–4.11 (m, 2H), 3.13–2.74 (m, 8H), 1.35 (s, 9H), 1.34 (s, 9H); ^{13}C NMR (300 MHz; DMSO-d_6) δ 173.3, 172.9, 156.4, 139.4, 137.2, 130.4, 129.2, 128.6, 127.3, 124.8, 122.0, 119.7, 119.3, 112.4, 111.5, 79.2, 57.0, 56.4, 39.5, 38.9, 29.3, 29.1; ESIMS m/z 594.1 [M+H]$^+$; FAB(+) m/z 594.4 [M+H]$^+$; HRMS calcd for $C_{32}H_{44}N_5O_6$ [M+H]$^+$: 594.3292, found 594.3285.

4.4.2. N-(2-{[N^6-[(Benzyloxy)carbonyl]-N^2-(tert-butoxycarbonyl)-L-lysyl]amino}ethyl)-N-(tert-butoxycarbonyl)-L-tryptophanamide (12)

Compound 11 (0.93 g, 2.20 mmol), 0.84 mL (4.84 mol) of DIEA, 0.74 g (2.42 mmol) of Boc-tryptophan, 0.65 (4.84 mmol) of HOBt and 1.26 g (2.42 mmol) of PyBOP in 40 mL DMF yielded 1.05 g (67%) of 12 as a white solid. Mp 157–160 °C; ^{1}H NMR (300 MHz; CDCl$_3$) δ 9.16 (br, 1H), 7.68 (d, 1H, J=6 Hz), 7.41–7.04 (m, 9H), 6.38 (br, 1H), 5.75 (br, 1H), 5.26 (br, 1H), 5.17–5.15 (m, 1H), 5.10 (s, 2H), 5.06–5.04 (m, 1H), 4.44 (br, 1H), 3.85–3.83 (m, 1H), 3.35–2.99 (m, 8H), 1.82–1.60 (m, 2H), 1.50–1.10 (m, 4H), 1.46 (s, 9H), 1.43 (s, 9H); ^{13}C NMR (300 MHz; CDCl$_3$) δ 173.1, 172.6, 157.1, 156.2, 155.8, 136,9, 136.6, 128.9, 128.5, 128.4, 127.8, 123.6, 122.6, 120.0, 119.4, 111,9, 111.1, 80.6, 80.4, 77.6, 67.1, 55.8, 54.5, 40.9, 39.8, 39.4, 32.6, 29.8, 29.2, 28.7, 28.7, 22.8; ESIMS m/z 709.5 [M+H]$^+$; FAB(+) m/z 709.6 [M+H]$^+$; HRMS calcd for $C_{37}H_{53}N_6O_8$ [M+H]$^+$: 709.3925, found 709.3906.

4.4.3. N-(tert-Butoxycarbonyl)-N-(2-{[N^2-(tert-butoxycarbonyl)-L-lysyl]amino}ethyl)-L-(tryptophanamide) (8)

A solution of 0.91 g of the Z-protected amine derivative 12 was prepared in 60 mL of methanol degassed with argon. Under a positive argon flow, 92 mg of Pd-black catalyst was slowly added to the

vigorously stirring degassed solution. After 6 h, the suspension was filtered through Celite. The Celite pad was washed with more methanol and the filtrate was concentrated under vacuum. The resultant residue was purified by column chromatography (silica, CH_2Cl_2/MeOH 3:1). Compound **8** (0.52 g, 70%) was obtained as a white solid. Mp 98–101 °C; ^{1}H NMR (300 MHz; CDCl$_3$) δ 9.54 (br, 1H), 7.75–7.72 (br, 1H), 7.45 (d, 1H, J=9 Hz), 7.26–7.07 (m, 4H), 5.35 (br, 1H), 5.15 (d, 1H, J=9 Hz), 4.38–4.33 (m, 1H), 3.76–3.71 (m, 1H), 3.37–3.14 (m, 4H), 2.95–2.78 (m, 2H), 2.52 (m, 2H), 1.86 (br, 2H), 1.60–0.8 (m, 6H), 1.47 (s, 9H), 1.45 (s, 9H); ^{13}C NMR (300 MHz; CDCl$_3$) δ 172.9, 172.4, 156.1, 155.7, 136.7, 127.8, 123.4, 122.6, 120.0, 119.2, 112.1, 111.4, 80.4, 80.2, 77.6, 55.7, 54.3, 41.1, 39.50, 38.7, 32.7, 30.9, 29.6, 28.7, 22.7; ESIMS m/z 575.2 [M+H]$^+$; FAB(+) m/z 575.5 [M+H]$^+$; HRMS calcd for $C_{29}H_{47}N_6O_6$ [M+H]$^+$: 575.3557, found 575.3549.

Acknowledgements

Supplementary data

^{1}H, ^{13}C NMR and ESI-MS spectra of synthesized compounds. Supplementary data associated with this article can be found in the online version, at doi:10.1016/j.tet.2009.07.031.

References and notes

1. Taylor, J. P.; Hardy, J.; Fischbeck, K. H. *Science* **2002**, *296*, 1991–1995.
2. Hardy, J.; Selkoe, D. J. *Science* **2002**, *297*, 353–356.
3. Nathalie, P.; Jean-Noel, O. *Curr. Alzheimer Res.* **2008**, *5*, 92–99.
4. Nerelius, C.; Johansson, J.; Sandegren, A. *Front Biosci.* **2009**, *14*, 1716–1729.
5. Hamley, I. W. *Angew. Chem., Int. Ed.* **2007**, *46*, 8128–8147.
6. Binder, W. H.; Smrzka, O. W. *Angew. Chem., Int. Ed.* **2006**, *45*, 7324–7328.
7. Maji, S. K.; Drew, M. G. B.; Banerjee, A. *Chem. Commun.* **2001**, 1946–1947.
8. Takahashi, T.; Mihara, H. *Acc. Chem. Res.* **2008**, *41*, 1309–1318.
9. Maezawa, I.; Hong, H. S.; Liu, R.; Wu, C. Y.; Cheng, R. H.; Kung, M. P.; Kung, H. F.; Lam, K. S.; Oddo, S.; LaFerla, F. M.; Jin, L. W. *J. Neurochem.* **2008**, *104*, 457–468.
10. Special Issue, *Acc. Chem. Res.* **2006**, *39*.
11. Stains, C. I.; Mondal, K.; Ghosh, I. *ChemMedChem* **2007**, *2*, 1674–1692.
12. Suh, J.; Yoo, S.; Kim, M.; Jeong, K.; Ahn, J. Y.; Kim, M. S.; Chae, P. S.; Lee, T. Y.; Lee, J.; Lee, J.; Jang, Y. A.; Ko, E. H. *Angew. Chem., Int. Ed.* **2007**, *46*, 7064–7067.
13. Cavalli, A.; Bolognesi, M. L.; Capsoni, S.; Andrisano, V.; Bartolini, M.; Margotti, E.; Cattaneo, A.; Recanatini, M.; Melchiorre, C. *Angew. Chem., Int. Ed.* **2007**, *46*, 3689–3692.
14. Bulic, B.; Pickhardt, M.; Khlistunova, I.; Biernat, J.; Mandelkow, E. M.; Mandelkow, E.; Waldmann, H. *Angew. Chem., Int. Ed.* **2007**, *46*, 9215–9219.
15. Rodríguez-Rodríguez, C.; Sánchez de Groot, N.; Rimola, A.; Álvarez-Larena, A.; Lloveras, V.; Vidal-Gancedo, J.; Ventura, S.; Vendrell, J.; Sodupe, M.; González-Duarte, P. *J. Am. Chem. Soc.* **2009**, *131*, 1436–1451.
16. Levine, H., III. *Amyloid* **2005**, *12*, 5–14.
17. Lockhart, A.; Ye, L.; Judd, D. B.; Merrittu, A. T.; Lowe, P. N.; Morgenstern, J. L.; Hong, G.; Gee, A. D.; Brown, J. *J. Biol. Chem.* **2005**, *280*, 7677–7684.
18. Lockhart, A. *Drug Discov. Today* **2006**, *11*, 1093–1099.
19. Ye, L.; Morgenstern, J. L.; Gee, A. D.; Hong, G.; Brown, J.; Lockhart, A. *J. Biol. Chem.* **2005**, *280*, 23599–23604.
20. Frid, P.; Anisimov, S. V.; Popovic, N. *Brain Res. Rev.* **2007**, *53*, 135–160.
21. Agdeppa, E. D.; Kepe, V.; Petric, A.; Satyamurthy, N.; Liu, J.; Huang, S. C.; Small, G. W.; Cole, G. M.; Barrio, J. R. *Neuroscience* **2003**, *117*, 723–730.
22. Weggen, S.; Rogers, M.; Eriksen, J. *Trends Pharmacol. Sci.* **2007**, *28*, 536–543.
23. Gasparini, L.; Ongini, E.; Wenk, G. *J. Neurochem.* **2004**, *91*, 521–536.
24. Hirohata, M.; Ono, K.; Naiki, H.; Yamada, M. *Neuropharmacology* **2005**, *49*, 1088–1099.
25. Gasparini, L.; Ongini, E.; Wilcock, D.; Morgan, D. *Brain Res. Rev.* **2005**, *48*, 400–408.
26. Coste, J.; Le-Nguyen, D.; Castro, B. *Tetrahedron Lett.* **1990**, *31*, 205–208.
27. Hoeg-Jensen, T.; Jakobsen, M. H.; Holm, A. *Tetrahedron Lett.* **1991**, *32*, 6387–6390.
28. Frérot, E.; Coste, J.; Pantaloni, A.; Dufour, M.-N.; Jouin, P. *Tetrahedron* **1991**, *47*, 259–270.
29. Becerril, J.; Bolte, M.; Burguete, M. I.; Galindo, F.; Garcia-España, E.; Luis, S. V.; Miravet, J. F. *J. Am. Chem. Soc.* **2003**, *125*, 6677–6686.
30. Becerril, J.; Burguete, M. I.; Escuder, B.; Galindo, F.; Gavara, R.; Miravet, J. F.; Luis, S. V.; Peris, G. *Chem.—Eur. J.* **2004**, *10*, 3879–3890.
31. Burguete, M. I.; Galindo, F.; Izquierdo, M. A.; Luis, S. V.; Vigara, L. *Tetrahedron* **2007**, *63*, 9493–9501.
32. Galindo, F.; Burguete, M. I.; Vigara, L.; Luis, S. V.; Kabir, N.; Gavrilovic, J.; Russell, D. A. *Angew. Chem., Int. Ed.* **2005**, *44*, 6504–6508.
33. Lakowicz, J. R. *Principles of Fluorescence Spectroscopy*, 3rd ed.; Springer: New York, NY, 2006.
34. Marme, N.; Knemeyer, J. P.; Sauer, M.; Wolfrum, J. *Bioconjugate Chem.* **2003**, *14*, 1133–1139.
35. Mátyus, L.; Szöllosi, J.; Jenei, A. *J. Photochem. Photobiol., B* **2006**, *83*, 223–236.
36. Doose, S.; Neuweiler, H.; Sauer, M. *ChemPhysChem* **2005**, *6*, 2277–2285.
37. Pedzinski, T.; Marciniak, B.; Hug, G. L. *J. Photochem. Photobiol., A* **2002**, *150*, 21–30.
38. Wang, Y. H.; Zhang, H. M.; Liu, L.; Liang, Z. X.; Guo, Q. X.; Tung, C. H.; Inoue, Y.; Liu, Y. C. *J. Org. Chem.* **2002**, *67*, 2429–2434.
39. Jimenez, M. C.; Pischel, U.; Miranda, M. A. *J. Photochem. Photobiol., C: Photochem. Rev.* **2007**, *8*, 128–142.
40. Burguete, M. I.; Izquierdo, M. A.; Galindo, F.; Luis, S. V. *Chem. Phys. Lett.* **2008**, *460*, 503–506.
41. Vaya, I.; Jimenez, M. C.; Miranda, M. A. *Tetrahedron: Asymmetry* **2005**, *16*, 2167–2171.
42. Velazquez, M. M.; Valero, M.; Rodriguez, L. J.; Costa, S. M. B.; Santos, M. A. *J. Photochem. Photobiol., B* **1995**, *29*, 23–31.
43. Perkampus, H.-H. *UV–Vis Atlas of Organic Compounds*, 2nd ed.; VCH: Weinheim, 1992; Vol. 2.
44. Baytekin, B.; Baytekin, H. T.; Schalley, C. A. *Org. Biomol. Chem.* **2006**, *4*, 2825–2841.
45. Fricke, H.; Gerlach, A.; Unterberg, C.; Wehner, M.; Schrader, T.; Gerhards, M. *Angew. Chem. Int. Ed.* **2009**, *48*, 900–904.
46. Mitkina, T.; Fedin, V.; Llusar, R.; Sorribes, I.; Vicent, C. *J. Am. Soc. Mass Spectrom.* **2007**, *18*, 1863–1872.
47. Alfonso, I.; Bolte, M.; Bru, M.; Burguete, M. I.; Luis, S. V.; Rubio, J. *J. Am. Chem. Soc.* **2008**, *130*, 6137–6144.
48. Bru, M.; Alfonso, I.; Burguete, M. I.; Luis, S. V. *Angew. Chem., Int. Ed.* **2006**, *45*, 6155–6159.
49. Zadmard, R.; Kraft, A.; Schrader, T.; Linne, U. *Chem.—Eur. J.* **2004**, *10*, 4233–4239.
50. Cockroft, S. L.; Perkins, J.; Zonta, C.; Adams, H.; Spey, S. E.; Low, C. M. R.; Vinter, J. G.; Lawson, K. R.; Urch, C. J.; Hunter, C. A. *Org. Biomol. Chem.* **2007**, *5*, 1062–1080.
51. Cockroft, S. L.; Hunter, C. A. *Chem. Soc. Rev.* **2007**, *36*, 172–188.
52. El-azizi, Y.; Schmitzer, A.; Collins, S. K. *Angew. Chem., Int. Ed.* **2006**, *45*, 968–973.
53. Meyer, E. A.; Castellano, R. K.; Diederich, F. *Angew. Chem., Int. Ed.* **2003**, *42*, 1210–1250.
54. Cozzi, F.; Annunziata, R.; Benaglia, M.; Cinquini, M.; Raimondi, L.; Baldridge, K. K.; Siegel, J. S. *Org. Biomol. Chem.* **2003**, *1*, 157–162.
55. Cozzi, F.; Cinquini, M.; Annunziata, R.; Dwyer, T.; Siegel, J. S. *J. Am. Chem. Soc.* **1992**, *114*, 5729–5733.
56. Reches, M.; Gazit, E. *Science* **2003**, *300*, 625–627.
57. Cherny, I.; Gazit, E. *Angew. Chem., Int. Ed.* **2008**, *47*, 4062–4069.
58. Azriel, R.; Gazit, E. *J. Biol. Chem.* **2001**, *276*, 34156–34161.
59. Porat, Y.; Mazor, Y.; Efrat, S.; Gazit, E. *Biochemistry* **2004**, *43*, 14454–14462.
60. Pawar, A. P.; DuBay, K. F.; Zurdo, J.; Chiti, F.; Vendruscolo, M.; Dobson, C. M. *J. Mol. Biol.* **2005**, *350*, 379–392.
61. Tjernberg, L. O.; Naslundt, J.; Lindqvist, F.; Johansson, J.; Karlstrom, A. R.; Thyberg, J.; Tereniust, L.; Nordstedt, C. *J. Biol. Chem.* **1996**, *271*, 8545–8548.
62. Petkova, A. T.; Yau, W. M.; Tycko, R. *Biochemistry* **2006**, *45*, 498–512.
63. Madine, J.; Jack, E.; Stockley, P. G.; Radford, S. E.; Serpell, L. C.; Middleton, D. A. *J. Am. Chem. Soc.* **2008**, *130*, 14990–15001.
64. Smith, T. J.; Stains, C. I.; Meyer, S. C.; Ghosh, I. *J. Am. Chem. Soc.* **2006**, *128*, 14456–14457.
65. Porat, Y.; Abramowitz, A.; Gazit, E. *Chem. Biol. Drug Des.* **2006**, *67*, 27–37.
66. Marek, P.; Abedini, A.; Song, B.; Kanungo, M.; Johnson, M. E.; Gupta, R.; Zaman, W.; Wong, S. S.; Raleigh, D. P. *Biochemistry* **2007**, *46*, 3255–3261.